Perpustakaan UAI

Improved S-bend optical waveguide loss formula verified by experiments

Improved S-bend optical waveguide loss formula verified by experiments

Permintaan Dosen [2026]

Universitas Al Azhar Indonesia

Document Details

Submission ID
trn:oid:::1:3699728801

Submission Date
Nov 3, 2026, 1:18 PM GMT+7

Download Date
Nov 5, 2026, 10:22 AM GMT+7

File Name
-bend_optical_waveguide_loss_formula_verified_by_experiments.pdf

File Size
2.0 MB

9 Pages

4,555 Words

23,578 Characters

10% Overall Similarity

The combined total of all matches, including overlapping sources, for each database.

Filtered from the Report

- Bibliography

Exclusions

- 23 Excluded Matches

Match Groups

11 Not Cited or Quoted 10%
Matches with neither in-text citation nor quotation marks

0 Missing Quotations 0%
Matches that are still very similar to source material

0 Missing Citation 0%
Matches that have quotation marks, but no in-text citation

0 Cited and Quoted 0%
Matches with in-text citation present, but no quotation marks

Top Sources

9% Internet sources
10% Publications
0% Submitted works (Student Papers)

Integrity Flags

0 Integrity Flags for Review

No suspicious text manipulations found.

Our system's algorithms look deeply at a document for any inconsistencies that would set it apart from a normal submission. If we notice something strange, we flag it for you to review.

A Flag is not necessarily an indicator of a problem. However, we'd recommend you focus your attention there for further review.

Match Groups

- **11** Not Cited or Quoted 10%
  Matches with neither in-text citation nor quotation marks
- **0** Missing Quotations 0%
  Matches that are still very similar to source material
- **0** Missing Citation 0%
  Matches that have quotation marks, but no in-text citation
- **0** Cited and Quoted 0%
  Matches with in-text citation present, but no quotation marks

Top Sources

9% Internet sources
10% Publications
0% Submitted works (Student Papers)

Top Sources

The sources with the highest number of matches within the submission. Overlapping sources will not be displayed.

1 Publication

Ary Syahriar. "Improved S-bend optical waveguide loss formula verified by experi... **8%**

2 Internet

pmc.ncbi.nlm.nih.gov **1%**

turnitin Page 4 of 12 - Integrity Submission www.nature.com/scientificreports Submission ID trn:oid:::1:3699728801

scientific reports

Check for updates

OPEN

Improved S-bend optical waveguide loss formula verified by experiments

Ary Syahriar

Curvature of a dielectric waveguide always leads to attenuation of the mode power as it propagates through the curved region. In single mode guides, bending loss becomes significant as the radius of curvature reduces and is strongly dependent on the confinement of the guided mode, so that weakly guiding waveguides can tolerate only large radii of curvature. In this paper we verify our new theoretical version on power loss prediction of S-bend optical waveguides by using analytical theory based on integration of absorption coefficient and compare it to the experimental measurement of such waveguide bends. The objectives are to formulate the best analytical theory available that can predict the power loss in S-bends whose shape is defined as a function $y=f(x)$, where its first derivative is continuous. Using this technique, the effect of post-process thermal annealing of channel guide devices fabricated by electron beam irradiation of silica PECVD materials is investigated. A particular performance characteristic is examined, which have its origin in the index reduction caused by annealing, increases in waveguide bend losses. Furthermore, to determine the waveguide shape, we used Marcatili's effective index method, employing model-dependent parameters obtained from the experimental data.

Optical waveguide bends are important devices in optical integrated circuits because it determines the overall performance of optical circuits built in single substrate. However, curved waveguides are known to increase losses as optical power propagates in the bend sections that lower the performance of overall optical waveguide system. Therefore, it is necessary to understand loss mechanism inside bend waveguides such as distortion of the transverse field profile, radiation loss, orthogonal polarization modes coupling and variation of the phase constant[1–3].

There are two important loss mechanisms[4]:

1. Loss due to radiation arising from the overall curvature of the waveguide (pure bending loss).
2. Loss due to transition at the junctions between bend region and straight input and output waveguides.

The magnitudes of pure bending losses have been analyzed with a variety of methods and a number of analytical formulae have been derived[5–9]. Pure bending loss may be explained as follows. As the fundamental mode enters the curved section, the fraction of the evanescent mode furthest from the center of curvature cannot travel sufficiently fast to keep in phase with the rest of the mode and therefore radiates away. As a result, the evanescent field must be continually resupplied with power obtained from the mode as it travels along the bending section, so that the overall amplitude of the mode must decrease with distance[10,11]. Decreasing the radius of curvature or increasing modal field confinement can reduce radiation loss. However, it will enlarge the overall device length and increase coupling loss when fibers optics are connected to the input and output of the optical circuits. Therefore, several different design alternatives on bends waveguides have been proposed to lessen the radiation loss which include, the use of an offset waveguide junction[6], an S-shaped curved waveguides[5–9] and an optimized continuous path[10]. Precision on these structures design requires accurate understanding of the mode changes as it enters the curved section. Transition loss arises mainly from the abrupt change in curvature experienced by the guided mode at the junction between a curved waveguide and a straight guide. This change introduces an offset between the modes of the straight and bends guides, which results in misalignment of the modal fields, and hence gives rise to further radiation loss. An established strategy to lower the transition loss is to shift the core of a straight guide relative to the waveguide bend axis at the end of the bend by a distance equal to the mode shift due to the curvature[12]. An alternative approach is to lessen the transition loss by employing a continuous variation of curvature from the straight waveguide to the desired value in the curved section. This approach

Department of Electrical Engineering, Faculty of Science and Technology, University Al Azhar Indonesia, Jakarta, Indonesia. email: ary@uai.ac.id

turnitin Page 4 of 12 - Integrity Submission Submission ID trn:oid:::1:3699728801

ensures that the fundamental mode propagates adiabatically along the transition region, so that at any particular value of curvature only pure bending loss can occur.

We concentrate on sinusoidal profile function $y=f(x)$, where its first derivative is continuous. Details analysis on analytical solution for such curved shape waveguide has been explained elsewhere[9]. In this paper we verify the previous analytical solution to the experimental results performed on S-bend channel guide devices fabricated by electron beam irradiation of silica PECVD material. The particular loss characteristics is examined which have their origin in the effective refractive index reduction caused by annealing. Additionally, by using this technique, the increase in waveguide bend losses caused by post process annealing can also be examined.

Waveguide bend geometries

In this section we consider continuously varying sinusoidal S-shaped curved waveguides. Figure 1 shows a schematic diagram of S-shaped curved waveguides length L connecting two parallel guides that are separated by a distance l, and a waveguide width of h.

The horizontal position $y(x)$ of the waveguide along the bends at a distance x is described by[5–9]:

$$y(x) = \frac{x\,l}{L} - \frac{l}{2\,\pi}\,\sin\left(\frac{2\,\pi x}{L}\right) \tag{1}$$

This transition function has been found effective in low loss bend waveguides since it eliminates discontinuity in the first and the second derivatives of the function. To find the radius of curvature of such a function, two different expressions are often used. The first expression is the mathematically exact radius of curvature, which is defined as[5]:

$$r(x) = \frac{(1+y'(x)^2)^{\frac{3}{2}}}{y''(x)} \tag{2}$$

Due to the presence of the radical, Eq. (2) is unfortunately too complicated for general use. As a result, an alternative 'low slope approximation' is often used instead; this can be obtained by assuming that $1+y'\,(x)^2 \approx 1$ in Eq. (2), so that:

$$r\,(x) \approx \frac{1}{y''\,(x)} \tag{3}$$

For the sinusoidal shape function of Eq. (1), the low-slope approximation is valid when $L>>l$ (usually apply to a weakly-confining waveguide), the 'low-slope approximation'[5] curvature $\frac{1}{r}$ is described by:

$$\frac{1}{r} \approx \frac{2\,\pi l}{L^2}\,\sin\left(\frac{2\pi\,x}{L}\right) \tag{4}$$

Equation (4) implies that the curvature of a sinusoidal curved waveguide is variable, with zero curvature at the input and output and a maximum curvature (and hence a minimum bend radius) at $x=L/4$ and $x=3L/4$. To calculate the loss along S-bend we firstly consider on using the attenuation coefficient α in a single-mode waveguides with constant radius of curvature as[1,11]:

$$\alpha = C_1 \exp\left(-C_2 r\right) \tag{5}$$

Here C_1 and C_2 are two waveguides constants which depend on the waveguide and on the optical mode shape. The C_1 coefficient is related to the difference between the propagation constant within the guide and the cladding refractive index n_2. Additionally, the C_1 coefficient is strongly model dependent, and so it can be used to calculate the guide shape and other parameters. The variation of α with r was also shown to be dominated by the value of C_2. The C_2 value also provides a method for characterizing mode confinement, which is useful when investigating techniques for reducing bend losses. C_2 is defined as[11]:

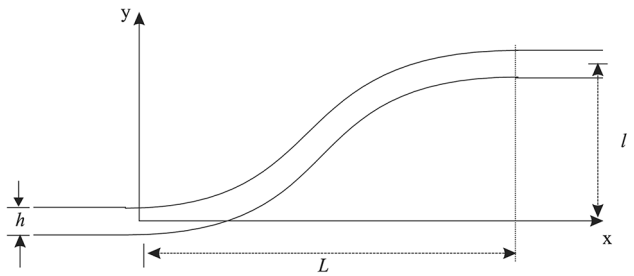


Fig. 1. S-shaped waveguide bend with a transition length L, a lateral offset l and a waveguide width of h.

$$C_2 = \frac{2\pi}{\lambda}\frac{(2\Delta n_{eff})^{\frac{3}{2}}}{\sqrt{n_2}} \tag{6}$$

Here $\Delta n_{eff} = n_{eff} - n_2$, where n_2 is the refractive index of the cladding. These results show that C_2 increases as the confinement becomes higher and also that C_2 values generally decrease slowly at long wavelengths. Then the total loss in dB is given by:

$$Loss = \frac{10}{\log_e(10)}\int_0^S \alpha(s)\ ds \tag{7}$$

where S represents the local position along the bend, $\alpha(s)$ is the attenuation coefficient at that point, and S is the bend waveguide total length. If Eq. (5) is substituted into Eq. (7) the total loss along the length of L is given by:

$$Loss = \left\{\frac{10}{\log_e(10)}\right\}\int_0^L C_1\ \exp(-C_2\, r(x))\ dx \tag{8}$$

Equation (8) can be used to calculate the total loss in sinusoidal S-bend profile where *r(x)* is given by Eq. (2) or (3). We now consider the development of analytical approximation to the line integral obtained in the low slope case. To do so, we proceed as follows. We start by assuming that Eq. (8) is valid and that the radius of curvature is given approximately by Eq. (4), the result is:

$$Loss = \left\{\frac{10}{\log_e(10)}\right\} C_1 \int_0^L \exp\left\{-\left(\frac{C_2 L^2}{2\pi h}\right)\frac{1}{\left|\sin\left(\frac{2\pi x}{L}\right)\right|}\right\} dx \tag{9}$$

To simplify Eq. (9), we now introduce some new dimensionless parameters. Defining the new parameters as $\gamma = \frac{C_2 L^2}{2\pi h}$ and $\theta = \frac{2\pi x}{L}$, Eq. (9) can then be transformed to[9]:

$$Loss = \left\{\frac{10}{\log_e(10)}\right\}\frac{C_1 L}{2\pi}\int_0^{2\pi} \exp\left\{\frac{-\gamma}{|\sin(\theta)|}\right\} d\theta \tag{10}$$

The task is now to evaluate the integral of Eq. (10). Unfortunately, no general analytical solution is known to exist to this equation either. However, two alternative methods may be used; the first is approximate analytical integration, while the second is parametric curve-fitting. For the approximate analytical integration, the result is[9]:

$$Loss = \left\{\frac{10}{\log_e(10)}\right\}\frac{C_1 L}{2\pi} 2\sqrt{\frac{2\pi}{\gamma}}\exp(-\gamma)\ erf\left(\sqrt{\frac{\gamma}{2}}\frac{\pi}{2}\right) \tag{11}$$

In this case the method of steepest decent has been used, and demonstrates that the total loss of a sinusoidal S-bend is dominated by the value of γ. This is because the approximations used are only valid for large γ, hence we expect Eq. (11) will be inaccurate when L is small, i.e. for short transition lengths. In 1982, Minford et al. published an entirely different analytical solution in the literature for loss in S-shape sinusoidal bend as[8]:

$$Loss = \frac{10}{\log_e(10)}\ 2\sqrt{2}\,\pi\frac{l}{L}\frac{C_1}{C_2}e^{-\gamma}\left[1 - e^{\frac{-\gamma}{2}}\right] \tag{12}$$

Equation (12) shows a passing resemblance to Eq. (11), especially in the exponential dependence of loss on the parameter γ. However, we have unable to validate the details of its mathematical derivation. Therefore, we have used 'brute force' method to get a closed form solution of Eq. (9), by using a parametric curve-fitting procedure to the result of direct numerical integration on low slope approximation. When this is done, the following expression on analytical solution was found to give the best agreement over the widest range of γ[9]:

$$Loss = \left\{\frac{10}{\log_e 10}\right\}\frac{C_1 L}{2\pi}\ \exp(-\gamma)\ \{3.5168 - 2.0843\log(\gamma)\} \tag{13}$$

We call this equation as the logarithmic curve-fitting function.

Verification with experiment measurements

In this section an attempt is made to fit these theoretical predictions with results obtained from experiments. For completeness, we consider fitting with four theoretical approximations of losses, namely, the low slope approximation using direct numerical integration (Eq. 9), the error function solution (Eq. 11), the exponential

turnitin Page 7 of 12 - Integrity Submission Submission ID trn:oid:::1:3699728801

analytic solution suggested by Minford et.al (Eq. 12), and the logarithmic curve-fit function(Eq. 13). In all cases, the devices were formed by electron beam irradiation of silica PECVD materials following the procedure described in[13–15]. These comprised of 32 μm layers of PECVD SiO_2, which were annealed prior to irradiation to convert the sign of index change due to irradiation effects[15]. Figure 2 shows a set of typical devices, which comprised straight waveguides, back-to-back S-bends, and Mach–Zehnder interferometers.

This picture was taken directly from the mask plate used to pattern the waveguide structures. Each S-bend has a constant lateral offset l and a different transition length L. The Mach–Zehnder interferometers were also constructed using similar sinusoidal bend shapes, which were simply reflected and overlaid one upon another to yield the desired interferometer structure.

In the experiments, all the waveguide bends were made with an offset of $l = 150$ μm and a transition length L varying between 1 and 6 mm. The overall chip length was 3.4 cm. The guide width of $h = 7$ μm was chosen close to single-mode optical fiber parameters as to get low loss coupling. The energy used for the irradiation was 25 keV, and the charge dose was 0.74 C/cm^2. The fiber-device-fiber insertion losses were measured with manually optimized butt-coupling between the fiber and the devices. The waveguides surface was covered by a layer of oil with a refractive index of 1.43.

Figure 3 shows measurements of TE and TM loss in waveguide bends made on PECVD material that had been subjected to two different treatments. The first sets of data were measured using material which had simply been irradiated. The second sets of measurements were made using a similar material, which was annealed in oxygen at 800 °C for 30 s after irradiation.

In each case, losses are relatively low at large transition lengths; rising abruptly as the transition length (and thus the minimum radius) is reduced. The transition length that may be tolerated is clearly lower after annealing. Figure 4a,b show a comparison of both sets of experimental data with a best fit to the low slope approximation of Eq. (9).

For $L > 4$ mm, the loss is essentially similar to the loss of a straight waveguide; however, as the transition length becomes smaller, the loss increases sharply. Furthermore, at some point where the radius of curvature becomes very small the loss tends to decrease. This is because the distance traveled round the bend is now very short, balancing the effect of an increasingly large value of α. The critical radius where the loss is maximum can be found by differentiating Eq. (5), as $r = 1/C_2$. In both cases, TE and TM loss differences appear which a result

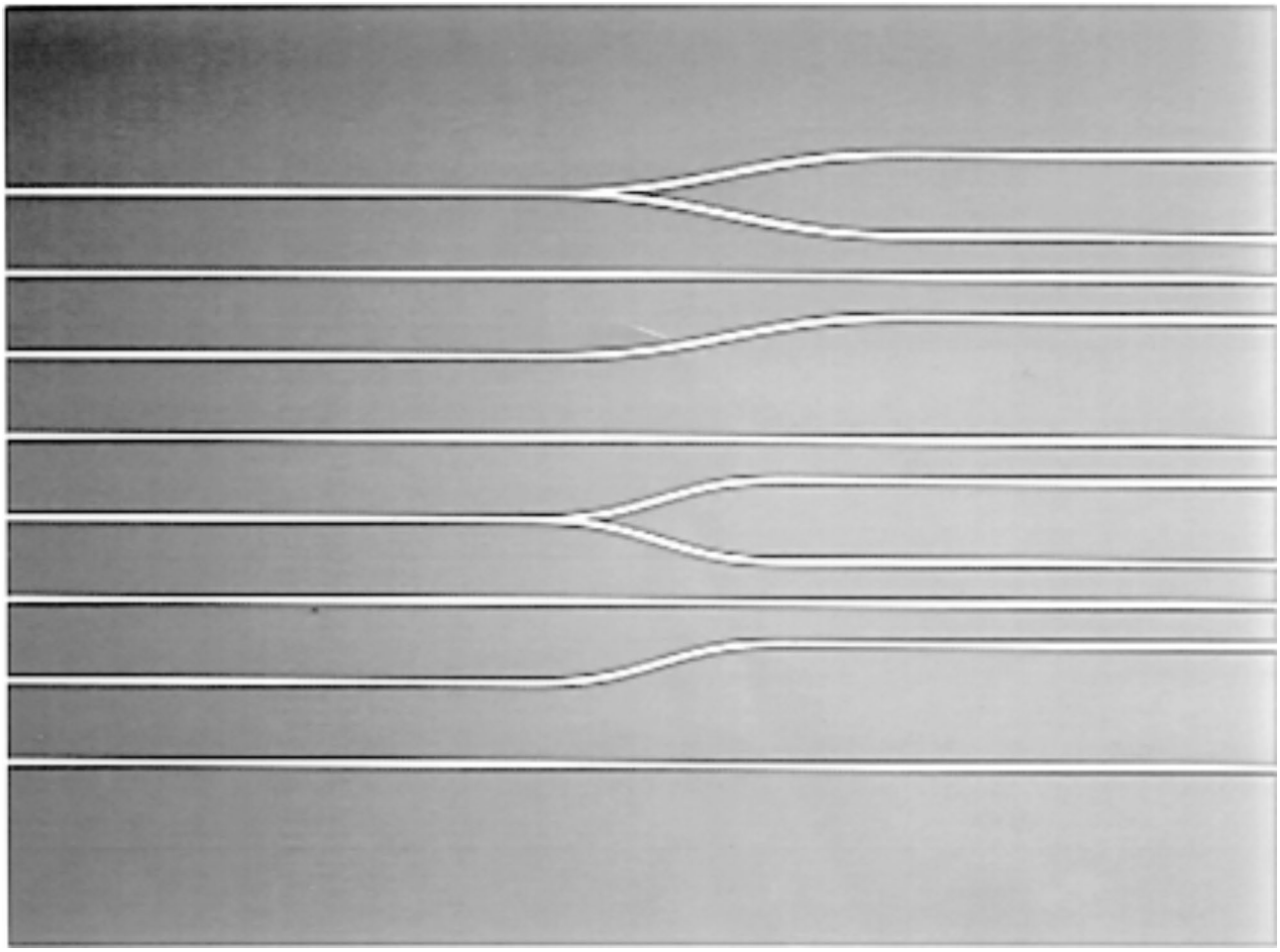


Fig. 2. Photograph of the mask used to generate the waveguide structures used in the experiments.

turnitin Page 7 of 12 - Integrity Submission Submission ID trn:oid:::1:3699728801

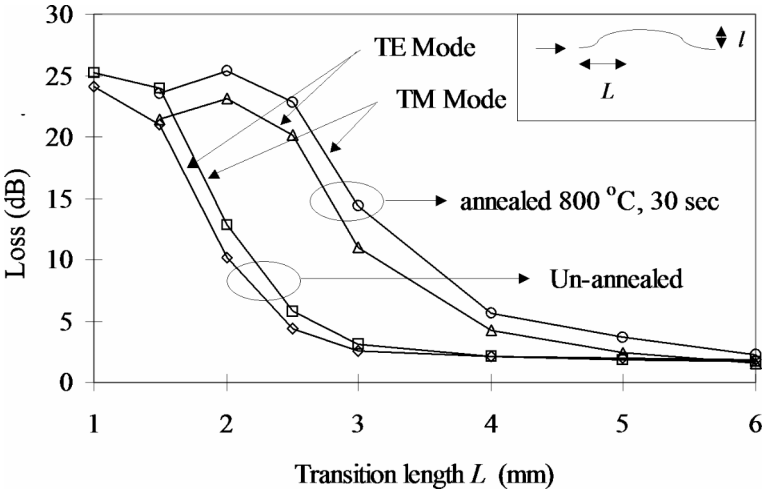


Fig. 3. The measurement of TE and TM loss of back-to-back S-bends of different transition lengths.

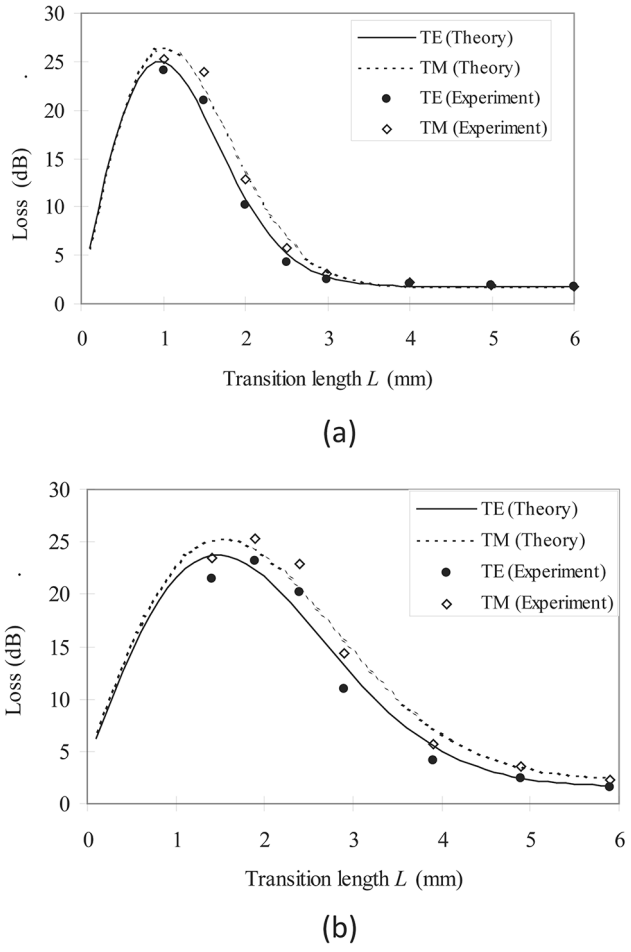


Fig. 4. Total loss of back-to-back S-bends of different lengths compared with the best fit to the low slope prediction, for two different treatments: (**a**) without annealing, (**b**) after annealing at 800 °C for 30 s.

of stress-induced birefringence is most likely. Furthermore, the asymmetry of core waveguides index profile and the use of low index cladding layer will also contribute to the differences[15]. The experimental data were fitted to the theoretical predictions as mentioned previously. For example, to perform matching with the low slope approximation, theoretical parameters of $\Delta n_{eff} = 1.19 \times 10^{-3}$ for the TE mode and $\Delta n_{eff} = 1.08 \times 10^{-3}$ for the TM

Mode	Functions	Δn_{eff} ($\times 10^{-3}$)	C_1 (m^{-1})	C_2 (m^{-1})
(TE)	Direct numerical integration (Eq. 9)	**1.19**	**5847.1**	**397.1**
	The error function solution (Eq. 10)	1.48	5082.7	552.3
	The exponential analytic solution (Eq. 11)	1.22	6518.8	416.2
	The logarithmic curve-fitting function (Eq. 12)	**1.21**	**6095.1**	**406.4**
(TM)	Direct numerical integration	**1.08**	**5760.1**	**347.2**
	The error function solution	1.40	4906.1	507.4
	The exponential analytic solution	1.13	6528.7	368.2
	The logarithmic curve- fitting function	**1.10**	**5981.7**	**354.6**

Table 1. The parameters Δn_{eff}, C_1 and C_2 for TE and TM modes obtained from guides fabricated by irradiation with no post-process annealing.

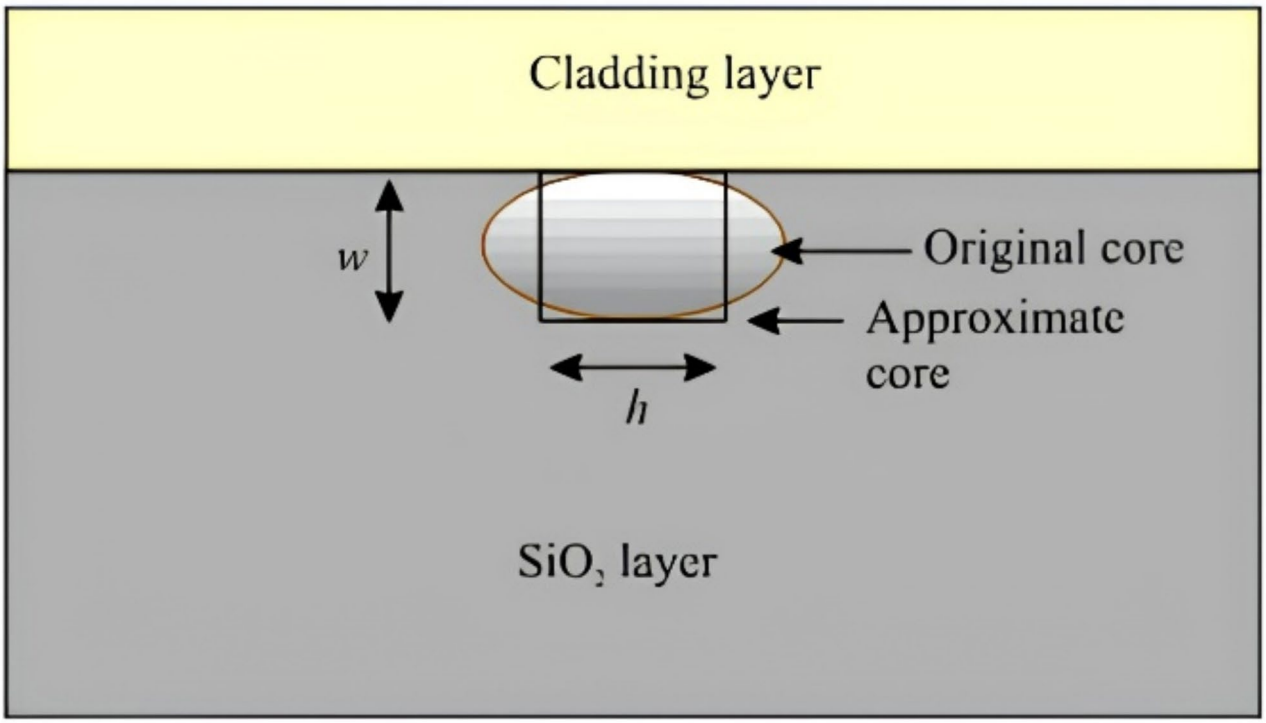


Fig. 5. An approximation to the graded-index irradiated waveguide core by a step-index rectangular core.

mode are required for the sample which was not annealed after irradiation. To investigate the validity of the bend loss theories described above, the experimental results are fitted to the four different theoretical approximations. In these fitting procedure we have used the values of $n_1 = 1.463$, $n_2 = 1.458$, $h = 7$ μm and the wavelength of $\lambda = 1.523$ nm. The first fit is performed on the un-annealed sample. A list of the fitted coefficients such as Δn_{eff}, C_1 and C_2 that were extracted from matching process using the four theoretical predictions is shown in Table 1.

Out all of the theoretical predictions, the low slope direct numerical integration is assumed to give the correct values for the Δn_{eff}, C_1 and C_2 coefficients. The error function solution, gives much higher Δn_{eff} and C_2 values but much lower C_1 coefficient when compared to the direct numerical integration. The exponential analytic solution, on the other hand, presents much higher Δn_{eff}, C_1 and C_2 values. Clearly, neither the error function nor the exponential analytic solution gives a good approximation. In fact, the closest agreement is obtained using the logarithmic curve-fitting function. This evidence suggests that the logarithmic curve-fitting function is indeed the best analytical solution, as anticipated previously[9].

Since the C_1 value is mainly related to the waveguide parameters, it may be used to determine the characteristic parameters of the guide, such as an effective core width and index. To do so, the effective index method developed by Marcatili is used to transform between a slab waveguide geometry and a three-dimensional guide[16,17]. In this analysis, it is assumed that irradiated waveguide has the shape of rectangular waveguide with a depth of ≈ 5 mm[15]. This shape may be approximated by a rectangular core as of uniform index shown in Fig. 5.

The calculation was done as follows. The Δn_{eff} value obtained from the matching process was used to obtain the effective waveguide width h using the method of bisection. The C_1 and C_2 coefficients were then calculated.

turnitin Page 10 of 12 - Integrity Submission Submission ID trn:oid:::1:3699728801

n_1	w (mm)	C_1 (m^{-1})	C_2 (m^{-1})
1.4606	5.6	12,427.6	397.7
1.46065	5.4	12,282.3	397.7
1.4607	5.3	12,149.6	397.7
1.46075	5.1	12,027.8	397.7
1.4608	5.0	11,919.5	397.7
1.46085	4.6	11,815.4	397.7

Table 2. A list of possible waveguide widths and the associated Δn_{eff}, C_1 and C_2 values calculated by using Marcatili's approaches[16].

Mode	Functions	Δn_{eff} ($\times 10^{-4}$)	C_1 (m^{-1})	C_2 (m^{-1})
(TE)	Direct numerical integration	**6.04**	**3260.2**	**143.1**
	The error function solution	11.74	3323.7	388.2
	The exponential analytic solution	8.61	4756.3	243.9
	The logarithmic curve-fitting function	**8.23**	**4190.4**	**227.6**
(TM)	Direct numerical integration	**5.69**	**3311.2**	**131.1**
	The error function solution	11.37	3502.4	370.1
	The exponential analytic solution	8.23	4931.8	227.8
	The logarithmic curve-fitting function	**7.81**	**4300.4**	**210.6**

Table 3. The Δn_{eff}, C_1 and C_2 parameters for TE and TM modes obtained from guides fabricated by irradiation, with post-process annealing.

The C_1 value obtained from each waveguide width was then compared with the experimental value. Generally, it was found that the two values were not compatible. For example, the calculated C_1 value was 12,427.6 m^{-1} with the parameters of $n_1 = 1.4606$ and $w = 5.6$ μm, while the experimental value is only 5847.1 m^{-1}. Table 2 shows a list of possible waveguide widths obtained from the Marcatili's method approaches, for $\lambda = 1.523$ mm, with the values of core refractive index n_1 varying from 1.4606 to 1.46085. As can be seen, the C_1 values are generally too high.

Similar C_1 values to those obtained from the experimental data were achieved, but only for very small (and hence unphysical) core widths. This disagreement might be due to the unsuitable choice of approximation by using a rectangular structure for the real shape of irradiated guide. Another possibility is that the shape of the refractive index variation of an irradiated core is simply too different from a step index function.

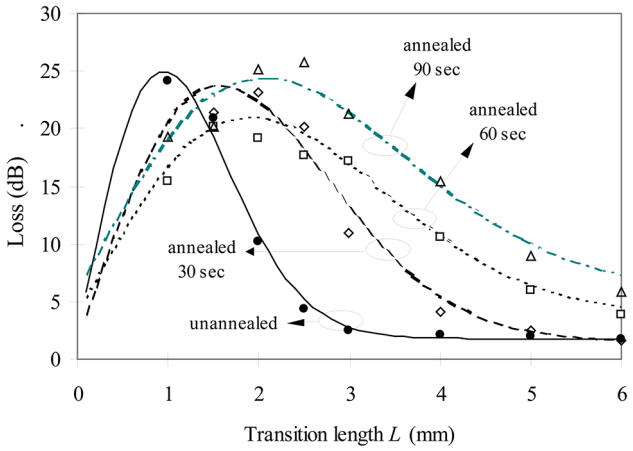
Similar comparisons between experiment and theory were also performed for the sample that had been annealed after irradiation. To achieve a good agreement, a value of $\Delta n_{eff} = 6.04 \times 10^{-4}$ was needed for the TE mode and $\Delta n_{eff} = 5.69 \times 10^{-4}$ for the TM mode, a substantial reduction. The four theoretical approximations were also applied to find the best fit. Table 3 shows the list of parameters obtained from the experimental data. From the best fit parameters, the logarithmic curve-fitting function gives the closest values to that of the low slope approximation results. This similarity reinforces the earlier conclusion that the logarithmic curve-fitting function gives the best approximation overall.

Figure 6a,b show TE and TM mode losses, obtained after annealing for different times, together with theoretical prediction of the logarithmic curve-fitting function. The loss tends to increase considerably even after post process annealing for a very short time. Clearly, the reason is a reduction in the refractive index difference forming the guide, resulting in lower confinement, so that the guided mode exhibits greater leakage into the cladding. Additionally, further annealing at high temperatures may have caused the waveguide width to increase, as the difference in the effective refractive index (Δn_{eff}) became smaller. This widening of the waveguide could lead to the excitation of higher-order modes, resulting in additional increased losses, likely due to the contribution of these higher modes. Furthermore, as the confinement is reduced, the mode is partially absorbed by silicon substrate which has index of refraction higher than silica. This effect can be determined from the TM mode losses, which are considerably higher than those of the TE mode. With longer annealing times the waveguide losses become proportionately higher and finally all guiding characteristic effectively disappears.

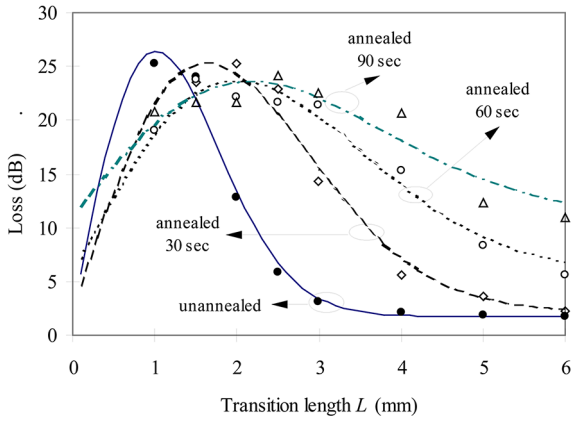
Conclusion

In conclusion, we have explored several approaches to calculating radiation loss in continuously-varying S-shaped waveguide bends. We examined the accuracy of different analytic approximations for the local loss coefficient in such bends and identified discrepancies between several previously published expressions. To assess the validity of these approaches, we compared four different analytic models against experimental data describing the cumulative loss in S-shaped waveguide structures. Our findings demonstrate that the previously published analytical solutions are inaccurate, and we show that an alternative logarithmic curve-fitting function provides significantly better accuracy across a wide range of parameters. This result supports the conclusion that the logarithmic curve-fitting function is the most accurate analytical approximation overall.

turnitin Page 10 of 12 - Integrity Submission Submission ID trn:oid:::1:3699728801



(a)



(b)

Fig. 6. Comparison of the loss characteristic of the sample after annealing: (a) TE mode, (b) TM mode. Points are experimental data; lines represent best theoretical fits.

Data availability

The data that support the findings of this study are available from the corresponding author upon reasonable request.

Received: 23 March 2024; Accepted: 23 December 2024
Published online: 08 January 2025

References

1. Marcatili, E. A. J. Bends in optical dielectric guides. *Bell Syst. Tech. J.* **48**, 2103–2132 (1969).
2. Song, J. H. et al. Low-loss waveguide bends by advanced shape for photonic integrated circuits. *J. Lightw. Technol.* **38**(12), 3273–3279 (2020).
3. Taylor, H. F. Power loss at directional change in dielectric waveguides. *Appl. Opt.* **13**, 642–647 (1974).
4. Ladouceur, F. & Love, J. D. *Silica-Based Buried Channel Waveguides and Devices* (Chapman & Hall, 1996).
5. Mustieles, F. J., Ballestores, E. & Baquero, P. Theoretical S-bend profile for optimisation of optical waveguide radiation losses. *IEEE Photon. Technol. Lett.* **5**, 551–553 (1993).
6. Baets, R. & Lagasse, P. E. Loss calculation and design of arbitrarily curved integrated-optic waveguides. *J. Opt. Soc. Am.* **73**, 177–182 (1983).
7. Marcuse, D. Length optimisation of an S-shaped transition between offset optical waveguides. *Appl. Opt.* **17**, 763–768 (1978).
8. Minford, W. J., Korotky, S. K. & Alferness, R. D. Low-loss Ti:$LiNbO_3$ waveguide bends at λ=1.3 μm. *IEEE J. Quantum Electron.* **QE-18**, 1802–1806 (1982).
9. Syahriar, A. A simple analytical solution for loss in S-bend optical waveguide. In *IEEE International RF and Microwave Conference* 357–360 (2008).
10. Ladouceur, F. & Labeye, P. A new general approach to optical waveguide path design. *IEEE J. Lightwave Technol.* **LT-13**, 481–492 (1995).
11. Lee, D. L. *Electromagnetic Principles of Integrated Optics* (Wiley, 1986).
12. Kitoh, T., Takato, N., Yasu, M. & Kawachi, M. Bending loss reduction in silica-based waveguides by using lateral offsets. *IEEE J. Lightwave Technol.* **LT-13**, 555–562 (1995).

13. Syms, R. R. A., Tate, T. J. & Lewandowski, J. J. Near-infrared channel waveguides formed by electron-beam irradiation of silica layers on silicon substrates. *IEEE J. Lightwave Technol.* **LT-12**, 2085–2091 (1994).
14. Lewandowski, J., Syms, R. R. A., Grant, M. & Bailey, S. Controlled formation of buried-channel waveguides by electron beam irradiation of glassy layers on silicon. *Int. J. Optoelectron.* **9**, 143–149 (1994).
15. Syms, R. R. A., Tate, T. J. & Bellerby, R. Low-loss near-infrared passive optical waveguide components formed by electron beam irradiation of silica-on-silicon. *IEEE J. Lightwave Technol.* **LT-13**, 1745–1749 (1995).
16. Marcatili, E. Dielectric rectangular waveguide and directional coupler for integrated optics. *Bell Syst. Tech. J.* **48**, 2071–2121 (Mar.1969).
17. Westerveld, W. J., Leinders, S. M., van Dongen, K. W. A., Urbach, H. P., & Yousef, M. Extension of Marcatili's analytical approach for, rectangular silicon optical waveguides. *IEEE J. Lightwave. Technol.* **30** (2012).

Acknowledgements
I would like to acknowledge on financial support partly from University al Azhar Indonesia

Author contributions
Ary Syahriar conceived the presented idea, developed the theory, performed the computation calculation, wrote the main manuscript and prepared Figures and Tables.

Declarations

Competing interests
The authors declare no competing interests.

Additional information
Supplementary Information The online version contains supplementary material available at https://doi.org/10.1038/s41598-024-84274-7.

Correspondence and requests for materials should be addressed to A.S.

Reprints and permissions information is available at www.nature.com/reprints.

Publisher's note Springer Nature remains neutral with regard to jurisdictional claims in published maps and institutional affiliations.

Open Access This article is licensed under a Creative Commons Attribution-NonCommercial-NoDerivatives 4.0 International License, which permits any non-commercial use, sharing, distribution and reproduction in any medium or format, as long as you give appropriate credit to the original author(s) and the source, provide a link to the Creative Commons licence, and indicate if you modified the licensed material. You do not have permission under this licence to share adapted material derived from this article or parts of it. The images or other third party material in this article are included in the article's Creative Commons licence, unless indicated otherwise in a credit line to the material. If material is not included in the article's Creative Commons licence and your intended use is not permitted by statutory regulation or exceeds the permitted use, you will need to obtain permission directly from the copyright holder. To view a copy of this licence, visit http://creativecommons.org/licenses/by-nc-nd/4.0/.

© The Author(s) 2025